Ageing effects on image sensors due to terrestrial cosmic radiation

Gayathri G. Nampoothiri [1], Marc L.R. Horemans [2], Albert J.P. Theuwissen [1, 3]
[1] Electronic Instrumentation lab, TU Delft, the Netherlands
[2] Consultant, Noorderwijk, Belgium
[3] Harvest Imaging, Bree, Belgium

ABSTRACT

We analyze the "ageing" effect on image sensors introduced by neutrons present in natural (terrestrial) cosmic environment. The results obtained at sea level are corroborated for the first time with accelerated neutron beam tests and for various image sensor operation conditions. The results reveal many fascinating effects that these rays introduce on image sensors.

Keywords: Ageing effects, Image sensors, Hot pixels, Radiation damage, Neutron irradiation.

1. INTRODUCTION

Gray hair and balding are considered to be the signs of ageing in humans! Imagers too exhibit a tendency to age which manifests as the generation of hard errors such as increase in hot pixels, increase in dark current, etc, even during on-the-shelf storage[1, 2]. These hot pixels are hard errors and are permanent unlike soft errors. Defects develop during the lifetime of imagers and do not disappear, limiting the imaging performance. It is hypothesized that the ageing phenomenon is due to the influence of terrestrial cosmic rays[3], which are the result of very high energy particles created in space or by the sun. These particles subsequently strike the earth's atmosphere. The energy and density of cosmic rays is dependant on altitude, latitude as well as the earth's magnetic field[4]. It is known that ceramic package, cover glass, adhesives, etc have little effect on the creation of hot pixels, even though they have effect on the generation of soft errors due to α-rays[5].

The energy of the cosmic ray is high enough to displace a silicon atom from its lattice position forming an interstitial vacancy pair. Typically energy of about 150 keV is needed to displace a silicon atom in the bulk lattice[6]. Most pairs recombine before they form a stable defect. The defects, in turn, interact with impurities to form defect-impurity complexes. These defects introduce additional energy levels in the forbidden band gap. Only around 2% of the initially generated vacancies remain[7].

Single event effects due to cosmic rays and the comparison between accelerated testing and high altitude measurements have been reported by[8]. In a previous work we have compared post-flight measurements at aviation altitudes to that of sea level and presented activation energy analysis of the sensors[9]. For the first time, these results are corroborated with neutron beam experiments to further understand underlying mechanisms. We also report the effect of dose rate and biasing on hot pixel generation.

[1] Email: g.gangadharannampoothiri@tudelft.nl

Sensors, Cameras, and Systems for Industrial, Scientific, and Consumer Applications XII,
edited by Ralf Widenhorn, Valérie Nguyen, Proc. of SPIE-IS&T Electronic Imaging, SPIE Vol. 7875,
78750G · © 2011 SPIE-IS&T · CCC code: 0277-786X/11/$18 · doi: 10.1117/12.871991

2. EXPERIMENTS

2.1 Setup and test device

An experimental setup capable of automated measurement and storage of data at regular intervals is developed (Figure 1). The measurement setup consists of a signal processing board, a sensor board capable of holding 16 imagers in parallel, a frame grabber and a laptop. Measurements are automated using LABView™ program. An uninterruptible power supply (UPS) ensures constant power to the devices. The experimental device used is a frame transfer Charge Coupled Device (CCD) measured as a full frame with an active area of 8.8 x 6.6 mm^2 and pixel size of 9 µm x 22 µm in the image section and 9 µm x 18.6 µm in the storage

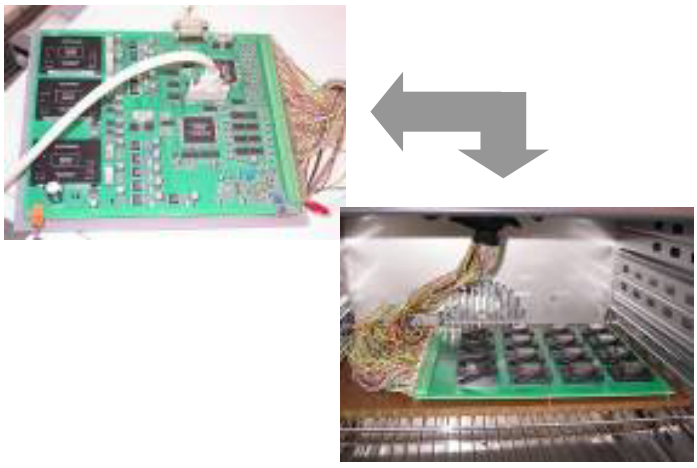

Figure 1: Signal processing board (top) and separate sensor board (bottom) housing 16 sensors in a temperature controlled oven.

.

2.2 Evaluation method

Measurements were done at regular intervals on reference sensors stored on-the-shelf at Delft, the Netherlands (52.01° N and 4.22° E) at room temperature. Temperature is recorded for each measurement and all measurements are done with an integration time of 3s. Another set of image sensors were irradiated in the ANITA (Atmospheric-like Neutrons from Thick Target) beam[10] at The Svedberg Laboratory (TSL), Sweden. Devices were irradiated at room temperature under biased conditions. Sensors were placed in the user position approximately 13.14m downstream of the ANITA target. Two different neutron flux settings were used: 200 ncm^{-2} s^{-1} and $1x10^4$ ncm^{-2} s^{-1} at the user position; energies above10 MeV. All measurements were done in the photo-sensitive region of the sensor. The amplitude of the pixel is expressed in digital numbers (DN). Pixels with values eight times higher than the standard deviation ($VI_{pix} \geq \delta\sigma_{pix}$) over the pixel array are marked out as hot pixels and their amplitudes recorded. This is repeated for all sensors at Delft and at TSL.

3. RESULTS AND DISCUSSION

Figure 2 show a 3D hot pixel map (pre-and post-neutron irradiation at TSL). Both measurements were carried out at a temperature of 22° C. Several new hot pixels can be perceived after the irradiation (obviously higher in count) similar to the results obtained due to natural exposure.

In order to check for any possible influence of dose rate during the accelerated tests, two groups of sensors received the same fluence but different flux. The result is shown in figure 3. Both the groups received a fluence of 10^6 ncm^{-2} with fluxes of 200 $ncm^{-2}s^{-1}$ and 10^4 $ncm^{-2}s^{-1}$ respectively. From the figure we can deduce that both the curves lie within the measurement error, and hence no influence of dose rate on measurements. Hence the use of accelerated testing for

comparison with the reference sensors is justified. In Figure 4 the effect of biasing on hot pixel generation is given. It is seen that biasing the sensor during irradiation increases the prospects of "lower amplitude" hot pixel generation by a factor of 2, and the effect drops for "higher amplitude" hot pixels, finally converging on the highest amplitudes. Figure 5 shows the effect of dose on the hot pixel generation. With respect to dose, the hot pixel count is seen to increase monotonically.

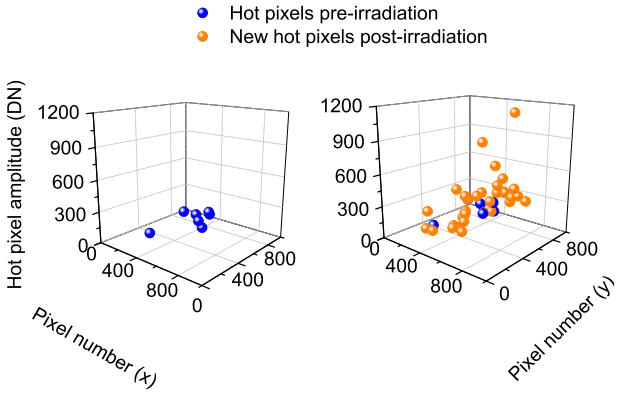

Figure 2: 3D hot pixel map from one sensor: (left) pre-irradiation and (right) post-neutron irradiation. Newly generated hot pixels are indicated.

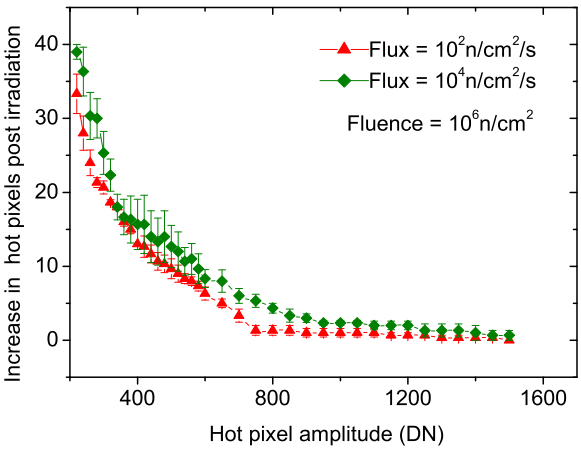

Figure 3 A comparison of the effect of neutron flux on hot pixel generation (average from measurement of 6 sensors). Both curves lie within measurement error.

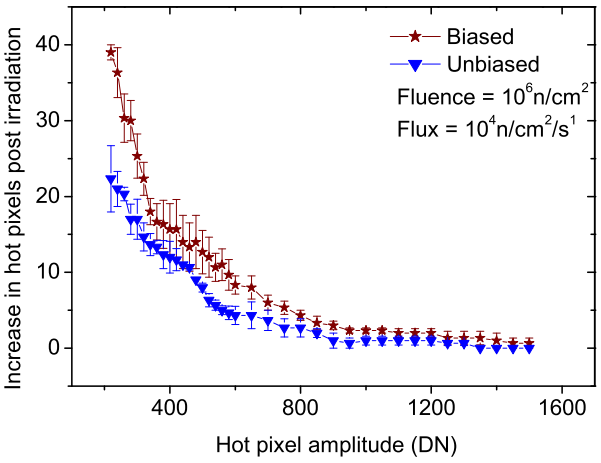

Figure 4 Effect of biasing on hot pixel generation (average from 6 sensors). Biasing increases the prospects of "lower amplitude" hot pixel generation by a factor of two. Effect is seen to drop for "higher amplitude" hot pixels.

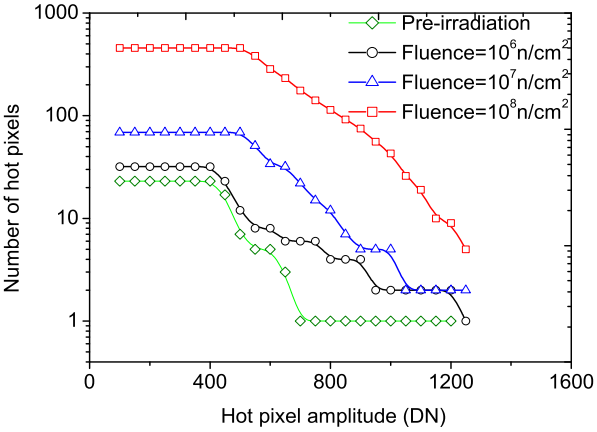

Figure 5 Hot pixel generation as a function of neutron fluence. An obvious step can be seen after irradiation.

Figure 6 compares neutron spectra at Delft, the Netherlands, and ANITA beam at TSL, Sweden. Spectrum at Delft was calculated using the *QinetiQ Atmospheric Radiation Model* (QARM) [11] assuming κ_ρ index of 3 and has been multiplied with a factor of 10^6 for comparison with TSL. ANITA spectrum was provided by the facility[12]. Figure 7 gives the comparison between reference sensors at the natural cosmic ray environment to sensors irradiated with neutrons using

ANITA beam at TSL. The X axis represents hot pixel amplitude expressed in digital numbers (DN). The two graphs are put on scale by normalizing the reference sensors (/day) and neutron irradiated sensors (/second). The curves reveal a similar hot pixel distribution pattern which provides further proof that neutrons in the cosmic rays are the major factor in the development of hot pixels.

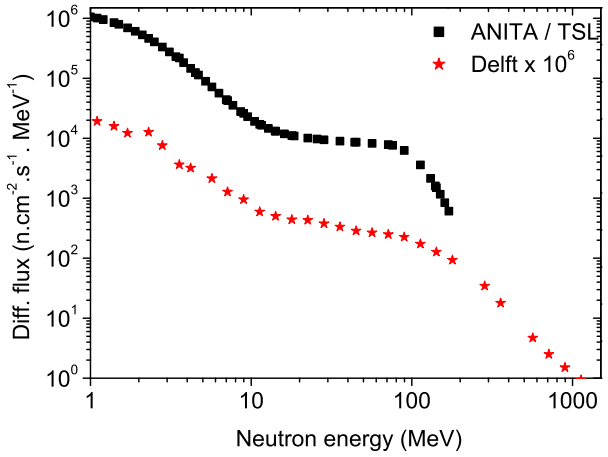

Figure 6 Neutron spectra at Delft and ANITA beam of TSL. ANITA neutron spectra provided by the facility. Delft spectra multiplied by a factor of 10^6 for comparison with ANITA/TSL.

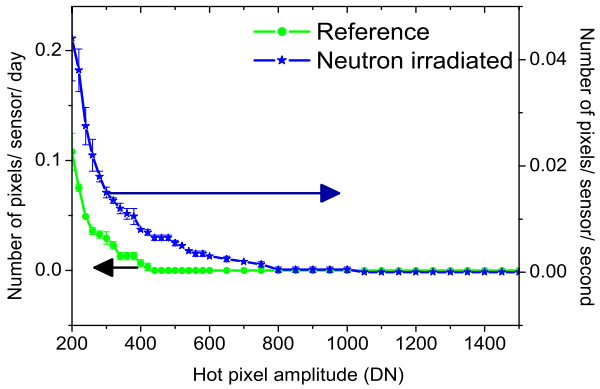

Figure 7 Comparison of reference sensors (natural cosmic ray environment) with neutron irradiated sensors (average data from 10 sensors). The similar pattern establishes terrestrial cosmic ray neutron as a major contributing factor in hot pixel development.

4. CONCLUSION

The effect of terrestrial cosmic radiation in the generation of hard errors resulting in hot pixels for solid sate image sensors has been studied. Hot pixel developments at sea level (terrestrial cosmic radiation environment) are corroborated successfully with accelerated neutron beam tests for the first time. Influence of neutron flux (dose rate) and biasing on hot pixel development is also reported. These experiments provide further validation to the hypothesis that the prominent cause of hot pixels is displacement damage in the silicon bulk due to neutron radiation, introduced by secondary cosmic rays.

ACKNOWLEDGMENT

The authors gratefully acknowledge the staff of the Svedberg Lab, Uppsala University, Sweden for enabling us to carry out the experiments; and DALSA for test devices. We like to thank Piet Trimp and Bernhard Buttgen (TU Delft) for help in the conduct of this research.

REFERENCES

[1] Hopkinson, G. et.al, "Proton effect in charge-coupled devices," IEEE Transactions on Nuclear Science., vol.43 (2), 614-627 (1996).
[2] Janesick, J., [Scientific Charge-Coupled Devices], SPIE Press, ISBN 0-8194-3698-4, 722-725 (2001).
[3] Theuwissen, A.J.P., "Influence of Terrestrial Cosmic Rays on the Reliability of Solid-State Image Sensors, Part I: Storage at Room Temperature", IEEE Transactions on Electron Devices, vol. ED-54, 3260-3266 (2007).
[4] Ziegler, J.F., "Terrestrial cosmic rays," IBM journal of research and development, vol.40 (1), 19-39 (1996).

[5] Dyer, C.S. et.al, "Cosmic radiation effects on avionics," Microprocessors and Microsystems, vol.22, 477-483 (1999).
[6] Janesick, J. et.al, "Radiation damage in Scientific Charge-Coupled Devices," IEEE Transactions on Nuclear Science, vol.36, 572-578 (1989).
[7] Van Lint, V.A.J., "The Physics of Radiation Damage in Particle Detectors," Nuclear Instr. Meth. Physics Res., vol.A253, 453-459 (1987).
[8] Török, Z., Platt, S.P. and Cai, X.X., "SEE-inducing effects of cosmic rays at the High-Altitude Research Station Jungfraujoch compared to accelerated test data," Proc. 9th European Conf. Rad. Effects. Compon. Syst. (RADECS), paper D-1 (2007).
[9] Gangadharan Nampoothiri, G., "Investigating the Ageing Effects on Image Sensors due to Terrestrial Cosmic Radiation," Proc. Of 2009 International Image Sensor Workshop, Bergen, Norway, June 22-28 (2009).
[10] Prokofiev, A.V. et.al, "ANITA a new neutron facility for accelarated SEE Testing at The Svedberg Laboratory," Proc. Int. Rel. Phy. Symp, 929-935 (2009).
[11] QinetiQ Atmospheric Radiation Model (QARM). [Online] Available: http://qarm.space.qinetiq.com/
[12] Prokofiev, A.V. et.al, "Characterization of the ANITA Neutron Source for accelarated SEE Testing at The Svedberg Laboratory," IEEE Radiation Effects Data Workshop, 166-173 (2009).